

MPC for Coupled Station Keeping, Attitude Control, and Momentum Management of GEO Satellites using On-Off Electric Propulsion

Zlotnik, D.; Di Cairano, S.; Weiss, A.

TR2017-129 August 2017

Abstract

This paper develops a model predictive control (MPC) policy for simultaneous station keeping, attitude control, and momentum management of a nadir-pointing geostationary satellite equipped with three reaction wheels and four on-off electric thrusters mounted on two boom assemblies attached to the anti-nadir face of the satellite. A closed-loop pulse-width modulation (PWM) scheme is implemented in conjunction with the MPC policy in order to generate on-off commands to the thrusters. The MPC policy is shown to satisfy all station keeping and attitude constraints while managing stored momentum, enforcing thruster constraints, and minimizing required delta-v.

IEEE Conference on Control Technology and Applications

This work may not be copied or reproduced in whole or in part for any commercial purpose. Permission to copy in whole or in part without payment of fee is granted for nonprofit educational and research purposes provided that all such whole or partial copies include the following: a notice that such copying is by permission of Mitsubishi Electric Research Laboratories, Inc.; an acknowledgment of the authors and individual contributions to the work; and all applicable portions of the copyright notice. Copying, reproduction, or republishing for any other purpose shall require a license with payment of fee to Mitsubishi Electric Research Laboratories, Inc. All rights reserved.

MPC for Coupled Station Keeping, Attitude Control, and Momentum Management of GEO Satellites using On-Off Electric Propulsion

David Zlotnik^{*}, Stefano Di Cairano[†], and Avishai Weiss[‡]

Abstract—This paper develops a model predictive control (MPC) policy for simultaneous station keeping, attitude control, and momentum management of a nadir-pointing geostationary satellite equipped with three reaction wheels and four on-off electric thrusters mounted on two boom assemblies attached to the anti-nadir face of the satellite. A closed-loop pulse-width modulation (PWM) scheme is implemented in conjunction with the MPC policy in order to generate on-off commands to the thrusters. The MPC policy is shown to satisfy all station keeping and attitude constraints while managing stored momentum, enforcing thruster constraints, and minimizing required delta-v.

I. INTRODUCTION

High specific impulse, low-thrust electric propulsion systems are increasingly being deployed on satellites for both interplanetary trajectories [1] and routine orbital maintenance [2], [3]. The increased propellant efficiency of electric thrusters relative to conventional chemical thrusters enables increased satellite lifetime and decreased propellant mass fraction, thereby lowering launch costs and facilitating larger payloads [4]. Electric propulsion systems must be operated on a near continuous basis, due to their comparatively low levels of thrust, and consequently render manual ground-based control impractical. Thus, autonomous closed-loop low-thrust station keeping control has garnered significant attention in recent years [5]–[11].

In [7], the authors use model predictive control (MPC) to treat the combined problem of geostationary Earth orbit (GEO) station keeping, nadir-pointing attitude control, and momentum management of a satellite equipped with four gimbaled electric thrusters placed directly on the satellite's anti-nadir face. This thruster arrangement, used also in [2], [9], [12], while more realistic than the authors' prior configuration in [6], hinders delta-v performance. The range of motion of the gimbals must be limited due to potential for plume impingement on North-South mounted solar panels. As North-South station keeping (NSSK), i.e. thrusting in the out-of-plane direction, is the dominant component in delta-v consumption, efficiency is sacrificed. Furthermore, the geometry of thrusters placed on the satellite's anti-nadir face results in their nominal torque-free angles, that is, the angles the thrusters are mounted so as to fire through the satellite's

center of mass, wasting much effort in the radial direction. Thus, the MPC policy of [7] often commands the gimbals to operate at their limits, generating undesirable torques on the satellite and unnecessarily burdening the reaction wheels, which due to limits on total angular momentum storage, results in additional delta-v being expended on momentum management. In this paper, the authors adapt the MPC policy in [7] to a satellite equipped with four electric thrusters mounted on two gimbaled boom assemblies attached to the anti-nadir face of the satellite. By introducing boom-thruster assemblies inspired by [13], the range of motion for efficient NSSK without risk of plume impingement is increased and the nominal torque-free angles result in less control effort being expended radially.

Additionally, the authors in [7] assume the ability to apply continuously variable thrust. While some advanced electric propulsion systems can throttle thrust magnitude [14], most systems remain on-off in nature, and thus [8]–[11] develop closed-loop station keeping control for on-off actuators. As such, one of the contributions of this paper is the development of a pulse-width modulation (PWM) scheme combined in closed-loop with an MPC policy that generates physically realizable on-off commands to thrusters mounted on gimbaled boom assemblies for simultaneous station keeping, attitude control, and momentum management.

The following notation will be used in all derivations. An arbitrary reference frame \mathcal{F}_a is a set of three orthonormal dextral basis vectors, $\{\underline{a}_1, \underline{a}_2, \underline{a}_3\}$. The vectors may be arranged in a vectrix $\underline{\mathcal{F}}_a$, where $\underline{\mathcal{F}}_a^T = [\underline{a}_1^T \ \underline{a}_2^T \ \underline{a}_3^T]$. An arbitrary vector \underline{v} may be resolved in \mathcal{F}_a as $\underline{v} = v_{a1}\underline{a}_1 + v_{a2}\underline{a}_2 + v_{a3}\underline{a}_3$ or alternatively as $\underline{v} = \underline{\mathcal{F}}_a^T \mathbf{v}_a$, where $\mathbf{v}_a = [v_{a1} \ v_{a2} \ v_{a3}]^T$ [15]. A vector may be resolved in any reference frame, for example, $\underline{v} = \underline{\mathcal{F}}_a^T \mathbf{v}_a = \underline{\mathcal{F}}_b^T \mathbf{v}_b$. The mapping between a vector resolved in \mathcal{F}_a to \mathcal{F}_b is given by the direction cosine matrix $\mathbf{C}_{ba} \in SO(3)$, $SO(3) = \{\mathbf{C} \in \mathbb{R}^{3 \times 3} \mid \mathbf{C}^T \mathbf{C} = \mathbf{I}, \det(\mathbf{C}) = +1\}$, such that $\mathbf{v}_b = \mathbf{C}_{ba} \mathbf{v}_a$. Principal rotations about the \underline{a}_i axis by an angle α are denoted by $\mathbf{C}_{ba} = \mathbf{C}_i(\alpha)$. The cross product between any two vectors can be expressed as $\underline{v} \times \underline{u} = \underline{\mathcal{F}}_a^T \mathbf{v}_a^\times \mathbf{u}_a$, where $(\cdot)^\times : \mathbb{R}^3 \rightarrow \mathfrak{so}(3)$, $\mathfrak{so}(3) = \{\mathbf{S} \in \mathbb{R}^{3 \times 3} \mid \mathbf{S} + \mathbf{S}^T = \mathbf{0}\}$. The operator $(\cdot)^V : \mathfrak{so}(3) \rightarrow \mathbb{R}^3$ is the inverse of $(\cdot)^\times$ such that $(\mathbf{v}_a^\times)^V = \mathbf{v}_a$. The anti-symmetric projection operator $\mathcal{P}_a(\cdot) : \mathbb{R}^{3 \times 3} \rightarrow \mathfrak{so}(3)$, is given by $\mathcal{P}_a(\mathbf{U}) = \frac{1}{2}(\mathbf{U} - \mathbf{U}^T)$, for all $\mathbf{U} \in \mathbb{R}^{3 \times 3}$. The vector describing the position of a point p relative to a point q is given by $\underline{r}_{\rightarrow p}^q$. Similarly, the angular velocity of frame \mathcal{F}_b relative to \mathcal{F}_a is given by $\underline{\omega}_{\rightarrow b}^{ba}$.

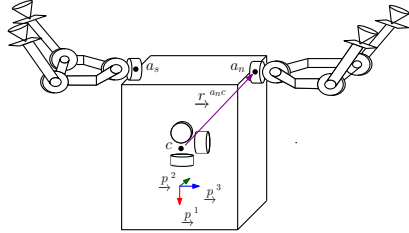
^{*}Ph.D. Candidate, Department of Aerospace Engineering, University of Michigan, Ann Arbor, MI 48109, USA. Email: dzlotnik@umich.edu. He was an intern at MERL during this development.

[†]Senior Principal Research Scientist, Mitsubishi Electric Research Laboratories, Cambridge, MA 02139, USA. Email: dicairano@merl.com

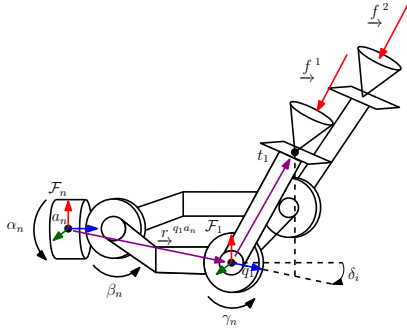
[‡]Research Scientist, Mitsubishi Electric Research Laboratories, Cambridge, MA 02139, USA. Email: weiss@merl.com

II. SPACECRAFT MODEL

The satellite model considered in this paper is shown in Fig. 1. Attached to the spacecraft bus is frame \mathcal{F}_p , where nominally \vec{p}^1 points to the center of the Earth and \vec{p}^3 points North. Point c denotes the center of mass of the spacecraft. The spacecraft mass is denoted m_B and the moment of inertia of the spacecraft relative to point c , resolved in frame \mathcal{F}_p , is $\mathbf{J}_p^{\mathcal{B}c}$. Reaction wheel speeds are denoted by $\dot{\gamma}$.



(a) Spacecraft model with reaction wheels



(b) North facing boom-thruster assembly.

Fig. 1: Spacecraft model including three axisymmetric reaction wheels and four electric thrusters. The first, second, and third axes of each reference frame are respectively denoted by red, green, and blue vectors. Frame \mathcal{F}_p is fixed to the spacecraft bus, while frames \mathcal{F}_n and \mathcal{F}_s determine the orientation of the assemblies relative to the bus.

The position of the spacecraft is described by position vector \vec{r}_g^{cw} which denotes the position of point c relative to point w , a point at the center of the Earth. The attitude of the spacecraft is given by the direction cosine matrix \mathbf{C}_{pg} , which describes the orientation of frame \mathcal{F}_p relative to the Earth-centered inertial (ECI) frame \mathcal{F}_g . The angular velocity of the spacecraft is ω_p^{pg} , that is the angular velocity of frame \mathcal{F}_p relative to \mathcal{F}_g resolved in \mathcal{F}_p . The equations of motion of the spacecraft are

$$\ddot{\vec{r}}_g^{cw} = -\mu \frac{\mathbf{r}_g^{cw}}{\|\mathbf{r}_g^{cw}\|^3} + \mathbf{a}_g^p + \frac{1}{m} \mathbf{C}_{pg}^T \mathbf{f}_p^{\text{thrust}}, \quad (1a)$$

$$\mathbf{J}_p^{\mathcal{B}c} \dot{\omega}_p^{pg} = -\omega_p^{pg \times} (\mathbf{J}_p^{\mathcal{B}c} \omega_p^{pg} + \mathbf{J}_s \dot{\gamma}) - \mathbf{J}_s \eta + \boldsymbol{\tau}_p^p + \boldsymbol{\tau}_p^{\text{thrust}}, \quad (1b)$$

$$\dot{\mathbf{C}}_{pg} = -\omega_p^{pg \times} \mathbf{C}_{pg}, \quad (1c)$$

$$\dot{\gamma} = \boldsymbol{\eta}, \quad (1d)$$

where $\boldsymbol{\eta}$ is the acceleration of the reaction wheels, \mathbf{J}_s is the moment of inertia of the reaction wheel array, and \mathbf{a}_g^p and

$\boldsymbol{\tau}_p^p$ are perturbations. The net force and torque produced by the thrusters are denoted by $\mathbf{f}_p^{\text{thrust}}$ and $\boldsymbol{\tau}_p^{\text{thrust}}$, respectively.

A. Thruster Configuration

The thruster configuration shown in Figs. 1a and 1b is considered. The four electric thrusters are paired in two boom-thruster assemblies attached to the anti-nadir face of the spacecraft. Points a_n and a_s denote the attachment points of the North and South facing assemblies. The North facing thruster assembly is depicted in Fig. 1b. At the base of the thruster assembly is a two degree of freedom gimbal, whose gimbal angles are α_n , β_n . Offset from the base are two thrusters, denoted thruster 1 and thruster 2, which apply forces at points t_1 and t_2 , respectively. The two thrusters can be simultaneously gimballed through a single degree of freedom by gimbal angle γ_n . Thrusters 3 and 4 are located on the South assembly, whose gimbal angles α_s , β_s , and γ_s are similarly defined. The thrusters are canted by fixed angles δ_i , $i \in \{1, 2, 3, 4\}$, such that for nominal gimbal angles, $\bar{\alpha}_a$, $\bar{\beta}_a$, and $\bar{\gamma}_a$, $a \in \{n, s\}$, each thruster fires through the center of mass of the spacecraft. Associated with thruster i on assembly a , is a frame \mathcal{F}_i such that $\vec{f}_i^i = \mathcal{F}_i^T \mathbf{f}_i^i$, where $\mathbf{f}_i^i = -f^i \mathbf{C}_2(\gamma_a) [0 \ 0 \ 1]^T$ and $f^i = \|\vec{f}_i^i\|$ is the magnitude of \vec{f}_i^i . In terms of γ_a and f^i , \mathbf{f}_i^i can be explicitly written as

$$\mathbf{f}_i^i = \begin{bmatrix} -\sin(\gamma_a) f^i & 0 & -\cos(\gamma_a) f^i \end{bmatrix}^T. \quad (2)$$

Resolved in frame \mathcal{F}_p , the thruster forces can be expressed as

$$\vec{f}_i^i = \mathcal{F}_p^T \mathbf{C}_{ip}^T \mathbf{f}_i^i = \mathcal{F}_p^T \mathbf{f}_p^i, \quad (3)$$

where $\mathbf{C}_{ip} = \mathbf{C}_{ia} \mathbf{C}_{ap}$, $\mathbf{C}_{ia} = \mathbf{C}_1(\delta_i) \mathbf{C}_2(\beta_a) \mathbf{C}_3(\alpha_a)$, $\mathbf{C}_{np} = \mathbf{C}_3(\pi)$, and $\mathbf{C}_{sp} = \mathbf{C}_1(\pi) \mathbf{C}_3(\pi)$. The torque that each thruster applies to the spacecraft is given by $\boldsymbol{\tau}_p^i = \mathbf{r}_p^{t_i c} \times \mathbf{f}_p^i$. Thus, the net force and torque produced on the spacecraft are given by

$$\mathbf{f}_p^{\text{thrust}} = \sum_{i=1}^4 \mathbf{C}_{ip}^T \mathbf{f}_i^i, \quad \boldsymbol{\tau}_p^{\text{thrust}} = \sum_{i=1}^4 \mathbf{r}_p^{t_i c} \times \mathbf{C}_{ip}^T \mathbf{f}_i^i. \quad (4)$$

III. MPC POLICY

The design of a controller which allows for the simultaneous station keeping, attitude control, and momentum management for the spacecraft described in the previous section is now considered. The control objectives are to:

- maintain the satellite in the station keeping window,
- maintain the satellite in a nadir pointing configuration,
- unload stored angular momentum in the reaction wheels,
- respect thruster magnitude and pointing limitations, and
- limit fuel consumption.

Following the previous works [6], [7], an MPC policy will be used to accomplish these objectives. Model predictive control generates control inputs by solving a receding-horizon finite-time optimal control problem based on a system model and a user-defined cost function [16]. It is highly desirable to formulate the MPC problem in terms of a linear time invariant system subject to linear constraints and a quadratic cost on the states and control inputs. Doing so allows for the

MPC problem to be formulated as a quadratic program (QP), which may be solved quickly and efficiently making it highly suitable for onboard implementation [6], [17]. Further, linear MPC is appropriate as the MPC policy keeps the spacecraft in a tight range about the equilibrium, where linearization introduces minimal errors.

In [7], it was observed that attitude constraint violations occurred when the MPC policy was allowed to control η . This was due to the high degree of nonlinearity associated with attitude control as well as the coupling between the orbital and attitude dynamics. As a solution, an inner-loop attitude controller was proposed in [7] to govern the reaction wheel accelerations while the MPC policy controlled the closed-loop satellite-attitude controller system. Here, we follow this general controller structure while considering the new thruster configuration described in Section II-A, and an updated control problem formulation that results in improvements of the control objectives.

A. Inner-Loop Attitude Controller

The non-adaptive form of the controller proposed in [18] and utilized in [7] is described here. First, it is assumed that the disturbance torque τ_p^p can be written as the output of the LTI system

$$\dot{\mathbf{x}}_d = \mathbf{A}_d \mathbf{x}_d, \quad \tau_p^p = \mathbf{C}_d \mathbf{x}_d. \quad (5)$$

Let $\hat{\tau}_p^p$ denote the estimate of τ_p^p and consider the following observer for τ_p^p ,

$$\dot{\hat{\mathbf{x}}}_d = \mathbf{A}_d \hat{\mathbf{x}}_d + \mathbf{B}_d \mathbf{u}_d, \quad \hat{\tau}_p^p = \mathbf{C}_d \hat{\mathbf{x}}_d, \quad (6)$$

where $\mathbf{u}_d = \omega_p^{pd} + \mathbf{K}_1 \mathbf{S}$, $\mathbf{K}_1 = \mathbf{K}_1^\top > 0$ is a constant, $\mathbf{S} = -\mathcal{P}_a(\mathbf{C}_{pd})^\vee$, and \mathbf{B}_d is designed such that (6) is positive real. As in [7], define

$$\begin{aligned} \nu_1 &= \omega_p^\times (\mathbf{J}_p \omega_p + \mathbf{J}_s \dot{\gamma}) - \mathbf{J}_p (\mathbf{K}_1 \dot{\mathbf{S}} + \omega_p^{pd \times} \omega_p) \\ \nu_2 &= -\hat{\tau}_p^p \\ \nu_3 &= -\mathbf{K}_\nu (\omega_p^{pd} + \mathbf{K}_1 \mathbf{S}) - \mathbf{K}_p \mathbf{S}. \end{aligned}$$

Then, the attitude controller proposed in [18] is $\eta = -\mathbf{J}_s^{-1}(\nu_1 + \nu_2 + \nu_3)$.

B. Linearization

Consider a linearization about a nominal circular orbit with mean motion n and a nadir pointing configuration with zero reaction wheel speeds. Letting $\bar{\mathbf{r}}_g$ denote the nominal position of the spacecraft in a circular orbit, the true position can be expressed as $\mathbf{r}_g^{cw} = \bar{\mathbf{r}}_g + \delta \mathbf{r}_g$, where $\delta \mathbf{r}_g$ is the position error of the spacecraft. Resolved in Hill's frame, \mathcal{F}_h , this error is given by $\delta \mathbf{r}_h = \mathbf{C}_{hg}(\mathbf{r}_g^{cw} - \bar{\mathbf{r}}_g)$. Hill's frame has \underline{h}^1 along the orbital radius, \underline{h}^2 orthogonal to \underline{h}^1 in the orbital plane, and \underline{h}^3 orthogonal to the orbital plane. A spacecraft in circular orbit with mean motion n has an angular velocity of $\bar{\omega}_p = [0 \ 0 \ n]^\top$. The angular velocity of the spacecraft can then be written as $\omega_p^{pg} = \bar{\omega}_p + \delta \omega$. Let \mathbf{C}_{dg} correspond to the desired value of \mathbf{C}_{pg} . The error between \mathbf{C}_{pg} and \mathbf{C}_{dg} is $\mathbf{C}_{pd} = \mathbf{C}_{pg} \mathbf{C}_{dg}^\top$. Let $\delta \theta = [\delta \phi \ \delta \theta \ \delta \psi]^\top$ denote the 3–2–1 Euler angle sequence associated with \mathbf{C}_{pd} , where $\delta \phi$,

$\delta \theta$, and $\delta \psi$ are errors in yaw, pitch, and roll, respectively. Substituting the above definitions into (1) gives the linearized equations of motion,

$$\begin{aligned} \delta \dot{\mathbf{r}}_h &= -2\omega_0^\times \delta \mathbf{r}_h - \mathbf{\Omega} \delta \mathbf{r}_h + \mathbf{a}_h^p + \frac{1}{m} \mathbf{C}_{dh}^\top \mathbf{f}_p^{\text{thrust}} \\ \delta \dot{\omega} &= [-\mathbf{K}_1 + \bar{\omega}_p^\times - \mathbf{J}_p \mathbf{K}_\nu] \delta \omega - \mathbf{J}_p^{-1} \mathbf{C}_d \hat{\tau}_p^p \\ &\quad + [\mathbf{K}_1 \bar{\omega}_p^\times - (\bar{\omega}_p^\times)^2 + \mathbf{J}_p^{-1} (\mathbf{K}_\nu \bar{\omega}_p^\times - \mathbf{K})] \delta \theta \\ &\quad + \tau_p^{\text{thrust}} \\ \ddot{\gamma} &= \eta \\ \dot{\mathbf{x}}_d &= \mathbf{A}_d \tilde{\mathbf{x}}_d + \mathbf{B}_d \delta \omega + \mathbf{B}_d (\mathbf{K}_1 - \bar{\omega}_p^\times) \delta \theta, \end{aligned}$$

where $\mathbf{K} = \mathbf{K}_\nu \mathbf{K}_1 + \mathbf{K}_p$, and $\mathbf{\Omega} = \text{diag}\{-3n^2, 0, n^2\}$.

As mentioned previously, it is desirable to formulate the MPC problem in terms of a linear time invariant system subject to linear constraints. To retain a linear system model it is assumed that α_a and β_a , $a \in \{n, s\}$, are fixed to their nominal values (i.e., $\alpha_a = \bar{\alpha}_a$ and $\beta_a = \bar{\beta}_a$), and the control inputs are selected as $\mathbf{u}_i = [\sin(\gamma_a) f^i \ \cos(\gamma_a) f^i]^\top$. Doing so allows $\mathbf{f}_p^{\text{thrust}}$ and τ_p^{thrust} to be written as $\mathbf{f}_p^{\text{thrust}} = \sum_{i=1}^4 \mathbf{B}_i^f \mathbf{u}_i$ and $\tau_p^{\text{thrust}} = \sum_{i=1}^4 \mathbf{B}_i^\tau \mathbf{u}_i$, where $\mathbf{B}_i^f = \mathbf{C}_{ip}^\top [-\mathbf{e}_1 \ -\mathbf{e}_3]$ and $\mathbf{B}_i^\tau = \mathbf{r}_p^{q_i \times} \mathbf{B}_i^f$ are constant matrices. Letting $\mathbf{x} = [\delta \mathbf{r}^\top \ \delta \dot{\mathbf{r}}^\top \ \delta \theta^\top \ \delta \omega^\top \ \dot{\gamma} \ \tilde{\mathbf{x}}_d]^\top$, $\mathbf{u} = [\mathbf{u}_1^\top \ \mathbf{u}_2^\top \ \mathbf{u}_3^\top \ \mathbf{u}_4^\top]^\top$, and $\mathbf{w} = [\mathbf{a}_h^{p \top} \ \mathbf{0} \ \mathbf{0} \ \mathbf{0} \ \mathbf{0} \ \mathbf{0}]^\top$, the discrete linear model with sampling period Δt is

$$\mathbf{x}_{k+1} = \mathbf{A}_d \mathbf{x}_k + \mathbf{B}_d \mathbf{u}_k + \mathbf{B}_w \mathbf{w}_k. \quad (7)$$

C. Constraints and MPC Formulation

The MPC problem must restrict the thruster forces to satisfy thruster magnitude as well as thruster pointing constraints. The thruster magnitude constraint is given by $\|\mathbf{f}_i^i\| \leq f_{\max}$, where f_{\max} is the maximum allowable thrust. This nonlinear magnitude constraint can be approximated by the linear constraint $|\mathbf{f}_i^i| \leq f_{\max}$. The pointing constraints are given by $\mathbf{f}_i^i \leq 0$, which ensures that the thrusters fire away from the spacecraft bus. These two constraints can be accomplished by enforcing

$$\mathbf{u}_i^{\min} \leq \mathbf{u}_i \leq \mathbf{u}_i^{\max}, \quad (8)$$

where $\mathbf{u}_i^{\max} = f_{\max} [1 \ 1]^\top$, $\mathbf{u}_i^{\min} = [0 \ 0]^\top$. In terms of \mathbf{u} , the control constraint is

$$\mathbf{u}_{\min} \leq \mathbf{u} \leq \mathbf{u}_{\max}, \quad (9)$$

where $\mathbf{u}_{\max} = [\mathbf{u}_1^{\max \top} \ \mathbf{u}_2^{\max \top} \ \mathbf{u}_3^{\max \top} \ \mathbf{u}_4^{\max \top}]^\top$ and $\mathbf{u}_{\min} = \mathbf{0}$. Recall that the two North and the two South facing thrusters are simultaneously driven by gimbal angles γ_n or γ_s . To formulate the MPC problem as a QP the constraint enforcing simultaneous gimbaling is neglected. Thus, the MPC policy may command inputs that require the thrusters to gimbal in non-physically realizable ways. However, this issue is removed by implementing a pulse-width modulation scheme, as will be explained later in Sec. IV.

Let λ_1 and λ_2 respectively denote the maximum allowable error in longitude and latitude. Then, the station keeping constraint can be expressed as $\delta \bar{\mathbf{r}}_{\min} \leq \delta \bar{\mathbf{r}} \leq \delta \bar{\mathbf{r}}_{\max}$, where $\bar{\mathbf{r}}_{\min} = [-\infty \ -\bar{r} \tan(\lambda_1) \ -\bar{r} \tan(\lambda_2)]$, $\bar{\mathbf{r}}_{\max} =$

$\begin{bmatrix} \infty & \bar{r} \tan(\lambda_1) & \bar{r} \tan(\lambda_2) \end{bmatrix}$ and $\bar{r} = \|\bar{\mathbf{r}}_g\|$ is the radius of the nominal circular orbit. Similarly, the attitude pointing constraints can be expressed as $\delta\theta_{\min} \leq \delta\theta \leq \delta\theta_{\max}$.

The MPC problem can be stated as follows,

$$\min_{\mathcal{U}_t} \mathbf{x}_{N|t}^\top \mathbf{P} \mathbf{x}_{N|t} + \sum_{k=0}^{N-1} \mathbf{x}_{k|t}^\top \mathbf{Q} \mathbf{x}_{k|t} + \mathbf{u}_{k|t}^\top \mathbf{R} \mathbf{u}_{k|t} \quad (10)$$

such that

$$\mathbf{x}_{k+1|t} = \mathbf{A}_d \mathbf{x}_{k|t} + \mathbf{B}_d \mathbf{u}_{k|t} + \mathbf{B}_{w,d} \mathbf{w}_{k|t},$$

$$\mathbf{x}_{0|t} = \mathbf{x}(t), \quad \mathbf{w}_{k|t} = \hat{\mathbf{w}}_t(t+k)$$

$$\mathbf{x}_{\min} \leq \mathbf{x}_{k|t} \leq \mathbf{x}_{\max},$$

$$\mathbf{u}_{\min} \leq \mathbf{u}_{k|t} \leq \mathbf{u}_{\max},$$

where N is the prediction horizon, $\mathcal{U}_t = \{\mathbf{u}_{0|t}, \dots, \mathbf{u}_{N-1|t}\}$, $\mathbf{Q} \geq 0$ and $\mathbf{R} > 0$ are state and control weights, and $\hat{\mathbf{w}}_i(j)$ is the open-loop predicted disturbance vector at time j based on data at time i [6]. The matrix $\mathbf{P} > 0$ is the terminal cost determined from the solution of the Discrete Algebraic Riccati Equation (DARE) for the infinite horizon problem. The control input is selected as $\mathbf{u}(t) = \mathbf{u}_{0|t}^*$, where $\mathbf{u}_{0|t}^*$ is the first element of \mathcal{U}_t^* , the minimizer of (10).

D. Simulation Results

The MPC policy developed in this section is tested in simulation against the nonlinear model of the orbital and attitude spacecraft dynamics (1), (4). Consider a spacecraft orbiting the Earth at geostationary altitude. The mass of the spacecraft is 4000 kg and each reaction wheel is 20 kg with a radius of 0.75 m and a height of 0.2 m. The base point of each thruster configuration is given by $\mathbf{r}_{p_n^c}^{a_n^c} = [-2 \ 0 \ 0.75]^\top$ m and $\mathbf{r}_{p_n^c}^{a_n^c} = [-2 \ 0 \ -0.75]^\top$ m. The boom-thruster assemblies have nominal configurations of $\bar{\alpha}_n = \bar{\alpha}_s = \bar{\beta}_n = \bar{\beta}_s = 0^\circ$ and $\bar{\gamma}_n = \bar{\gamma}_s = 40.14^\circ$ with $\mathbf{r}_{n_1^{a_n}}^{q_1^{a_n}} = \mathbf{r}_{n_3^{a_n}}^{q_3^{a_n}} = [0 \ 0.75 \ 1.5]^\top$ m and $\mathbf{r}_{n_2^{a_n}}^{q_2^{a_n}} = \mathbf{r}_{n_4^{a_n}}^{q_4^{a_n}} = [0 \ -0.75 \ 1.5]^\top$ m. A disturbance torque, $\boldsymbol{\tau}_s^p$, due to solar radiation pressure is included in the simulation. The perturbation torque is given in [19, p. 229], calculated assuming a mean surface area of 200 m², surface reflectance $c_{\text{refl}} = 0.6$, solar facing area $S_{\text{facing}} = 37.5$ m², and solar radiation pressure constant $C_{\text{srp}} = 4.5 \times 10^{-6}$ N/m². Acceleration perturbations, \mathbf{a}_p^p , due to Earth's oblateness, solar and lunar gravitational attraction, and solar radiation pressure are included and are calculated as in [6].

The initial spacecraft attitude is in a nadir pointing configuration with initial angular velocity $\boldsymbol{\omega}_p^{pg}(0) = \bar{\boldsymbol{\omega}}_p$ and zero initial reaction wheel speeds. For the MPC problem, the horizon is $N = 15$, the weighting matrices for each state are $\mathbf{Q}_r = 10^{-3} \text{diag}\{0, 1, 1\}$, $\mathbf{Q}_\theta = \mathbf{Q}_\omega = 10^{-3} \cdot \mathbf{I}$, $\mathbf{Q}_r = \mathbf{0}$, $\mathbf{Q}_{\bar{x}_d} = \mathbf{0}$, $\mathbf{Q}_{\bar{\gamma}} = 10^{-2} \cdot \mathbf{I}$, with $\mathbf{Q} = \text{diag}\{\mathbf{Q}_r, \mathbf{Q}_r, \mathbf{Q}_\theta, \mathbf{Q}_\omega, \mathbf{Q}_{\bar{\gamma}}, \mathbf{Q}_{\bar{x}_d}\}$.

The control weight \mathbf{R} is selected as $\mathbf{R} = \mathbf{R}_{\text{thrust}} + \mathbf{R}_{\text{torque}}$ where $\mathbf{R}_{\text{thrust}} = 10^4 \cdot \mathbf{I}$ and $\mathbf{R}_{\text{torque}} = 10^4 \mathbf{L}^\top \mathbf{L}$, $\mathbf{L} = \text{diag}\{\mathbf{B}_1^\top, \mathbf{B}_2^\top, \mathbf{B}_3^\top, \mathbf{B}_4^\top\}$. In this way, $\mathbf{u}^\top \mathbf{R} \mathbf{u} = 10^4 \sum_{i=1}^4 f_i^2 + 10^4 \sum_{i=1}^4 \tau_i^2$, where $\tau_i = \|\mathbf{r}_{p_i^c}^{q_i^c} \times \mathbf{f}_p^i\|$ is the norm of the torque produced by thruster i . By heavily penalizing torque

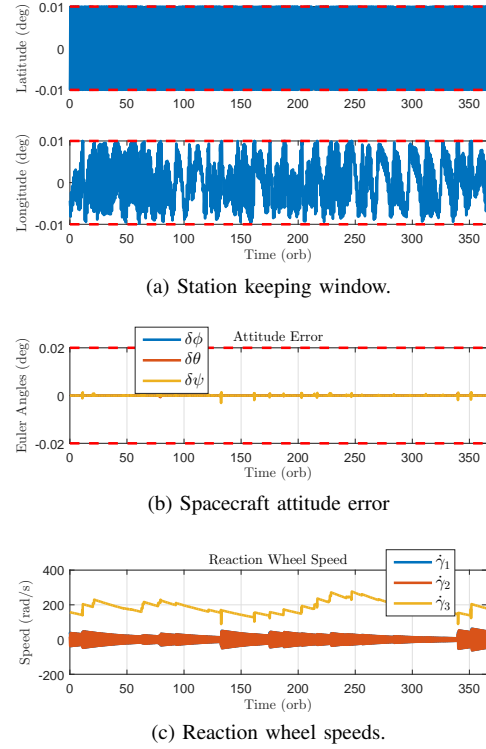


Fig. 2: Simulation over a period of one year.

in the MPC problem, the effects of undesirable torques on the spacecraft can be minimized.

Regarding the attitude controller, the controller gains are selected as $\mathbf{K}_1 = 0.2 \cdot \mathbf{I}$, $\mathbf{K}_p = 2 \cdot \mathbf{I}$, and $\mathbf{K}_v = 100 \cdot \mathbf{I}$. The matrices \mathbf{A}_d and \mathbf{C}_d are chosen as $\mathbf{A}_d = \text{diag}\{\bar{\mathbf{A}}_d, \bar{\mathbf{A}}_d, \bar{\mathbf{A}}_d\}$ and $\mathbf{C}_d = \text{diag}\{\bar{\mathbf{C}}_d, \bar{\mathbf{C}}_d, \bar{\mathbf{C}}_d\}$, where

$$\bar{\mathbf{A}}_d = \begin{bmatrix} -0.001 & -\omega_d^2 \\ 1 & -0.001 \end{bmatrix}, \quad (11)$$

$\omega_d = 2\pi$ rad/day, and $\bar{\mathbf{C}}_d = [1 \ 0]$. The matrix \mathbf{B}_d is chosen by picking $\mathbf{Q}_d = 0.001 \cdot \mathbf{I}$ solving $\mathbf{A}_d^\top \mathbf{P}_d + \mathbf{P}_d \mathbf{A}_d = -\mathbf{Q}_d$ for \mathbf{P}_d and setting $\mathbf{B}_d = \mathbf{C}_d^\top \mathbf{P}_d^{-1}$ [7].

The spacecraft is simulated for 425 days. The maximum thruster magnitude is set to $f_{\text{max}} = 0.1$ N. The station keeping window is $\pm 0.01^\circ$ in both latitude and longitude, while the maximum allowable attitude error is $\pm 0.02^\circ$ for yaw, pitch, and roll. The sampling period is $\Delta t = 1$ hour.

The total simulation time is 425 days, however, to avoid accounting for the (favorable) transient due to the initial position of the spacecraft, and to isolate the steady state periodic operation of the system, only the last 365 days of the simulation are used. Referring to Fig. 2a and Fig. 2b all constraints associated with station keeping and attitude are satisfied. Reaction wheel speeds are plotted in Fig. 2c, where it can be seen that the reaction wheel speeds remain bounded. This indicates that the MPC policy is able to successfully unload stored angular momentum.

The thruster force magnitudes, f_i^i , and gimbal angles, γ_a^i , over the last 5 orbits are plotted in Figs. 3a and 3b. The MPC

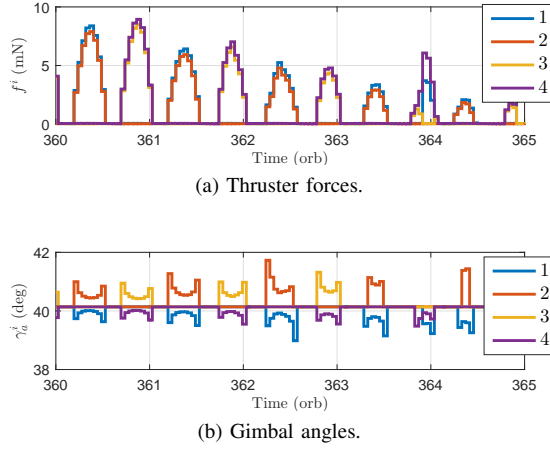


Fig. 3: Time histories of thruster magnitudes and gimbal angles over the last 5 days.

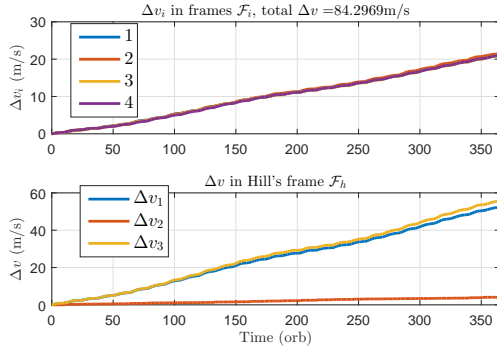


Fig. 4: Accumulation of Δv .

policy tends to alternate between simultaneously firing either the two North thrusters or the two South thrusters within an orbit, consistent with correcting for orbital inclination changes in NSSK. While in Figs. 3a and 3b the gimbal angles γ_i are selected independently, in reality on each boom-thruster assembly these are simultaneously driven and hence not independent. The PWM scheme in IV will rectify these non-physically realizable control commands.

The accumulation of Δv over a one year period, by each thruster and due to the net thrust resolved in \mathcal{F}_h , is shown in Fig. 4. The total annual Δv required by the MPC policy is about 84.3 m/s. To compare to previous results it will be useful to determine the portion of Δv spent on station keeping and the portion spent on momentum management. It is well known that the vast majority of annual Δv required for station keeping is accumulated in the out-of-plane \underline{h}^3 direction to counteract large out-of-plane perturbations. In a previous simulation considering station keeping only it was determined that about 55 m/s was required in the out-of-plane direction. Thus, an estimate of the amount of Δv necessary for station keeping only can be found by determining the amount of thrust required by the thrusters, in their nominal configuration, to produce $\Delta v_3 = 55$ m/s. The component of the force produced by thruster i in direction \underline{p}_i^3 , which

aligns with \underline{h}^3 in the nominal attitude configuration, is nominally given by $f_{p,3}^i = -\cos(\delta_i)\cos(\bar{\gamma}_a)f^i$ for North facing thrusters 1 and 2 and $f_{p,3}^i = \cos(\delta_i)\cos(\bar{\gamma}_a)f^i$ for South facing thrusters 3 and 4. Thus, to achieve the required Δv necessary for station keeping an increase in thruster magnitude by a factor of $(\cos(\delta_i)\cos(\bar{\gamma}_a))^{-1} = 1.3789$ is expected. Consequently, an estimate of the total Δv for station keeping is 75.8 m/s. The remaining 8.5 m/s is used to manage the reaction wheel speeds as well as East-West station keeping. Comparing this to a previous result in [7], a reduction of 16.67 m/s in total accumulated Δv is observed along with a reduction of 14.5 m/s in the Δv required for momentum management, due to the new thruster configuration and to changes in the cost function in (10).

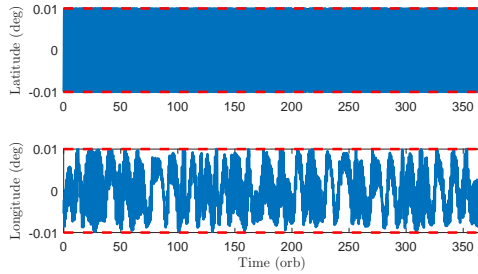
The effect of penalizing torque in the objective function can be observed by repeating the simulation with $\mathbf{R}_{\text{torque}} = \mathbf{0}$. Doing so results in a yearly Δv accumulation of 87.35 m/s. Assuming again that 75.8 m/s of Δv is used for station keeping, the remaining 11.55 m/s is used for East-West station keeping and momentum management. Removing the torque waiting in (10), causes an increase of 3.05 m/s in consumption for reaction wheels momentum dumping. This increase is due to the fact that when the thrusters produce torques on the spacecraft the reaction wheels act to maintain the spacecraft in a nadir pointing configuration. As a result, the stored angular momentum in the reaction wheels increases and fuel consumption increases due to subsequent momentum unloading.

IV. THRUSTER QUANTIZATION

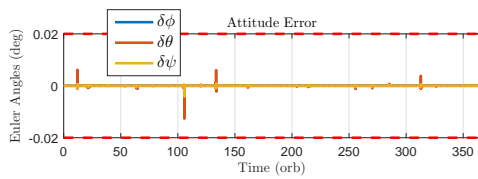
In the previous section it was assumed that all thrusters could fire simultaneously and that the thruster magnitudes could vary smoothly between zero and f_{max} . This is impractical for several reasons. First, each thruster is in reality an on-off actuator taking a value of either 0 or f_{max} at any time instant. Second, power limitations may limit the number of thrusters that can be on at the same time, and very often it is desirable to have only one thruster active at a time.

To remedy these problems, a method for quantizing the thrust requested by the MPC policy is developed and tested in this section. This is done by implementing a simple pulse-width modulation (PWM) scheme. The command from the MPC policy is constant over every 1 hour time period. During each hour active thrusters will pulse a total of N_p times. The length of each pulse must be such that the average thrust produced is equal to the constant thrust requested by the MPC policy. Let $T = \Delta t/N_p$, $\Delta t = 1$ hr, be the period of the PWM scheme. Assume the thruster fires at the beginning of each period. The cut-off time t_c is the time during the PWM period when the thruster is on. This can be calculated as $t_c = u_{\text{mpc}}T/u_{\text{max}}$, where u_{mpc} is the thrust commanded by the MPC policy. If the MPC policy requests more than one active thruster, the thrusters will fire consecutively (i.e., if thruster 1 fires at time $t = 0$, thruster 2 fires at $t = t_{c1}$ and cuts off at time $t = t_{c1} + t_{c2}$, etc.). The MPC policy and thruster quantization act in closed-loop, which is to say that MPC thruster commands are recalculated

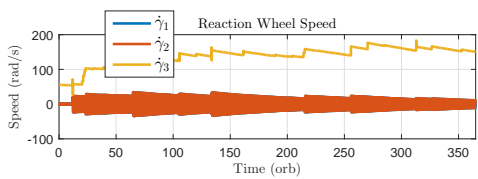
after every sampling period while only quantized thrust is implemented. This is a simple quantization scheme that is meant to demonstrate the feasibility of coupled MPC and thruster quantization.



(a) Station keeping window.



(b) Spacecraft attitude error



(c) Reaction wheel speeds.

The MPC policy with quantized thrust is now tested using the same parameters as in Sec. III-D. The number of pulses in one hour is set to $N_p = 5$. The simulation is over a period of 425 days, while only the last 365 days are shown. Referring to Fig. 5a, the spacecraft is able to remain mostly within the station keeping window. The attitude errors and reaction wheel speeds are plotted in Fig. 5b and Fig. 5c, respectively. The MPC policy coupled with the PWM scheme manages to keep the spacecraft attitude within the allowable attitude error limit. As in Sec. III, the reaction wheel speeds remain bounded, indicating that the control system is able to successfully unload stored angular momentum. During the simulation, the total Δv accumulated over a period of 365 days was 79.82 m/s. This indicates not only that the fuel consumption is not significantly degraded, but it may even be improved, possibly due to a finer actuator control with a period smaller than the MPC sampling period.

V. CONCLUSION

The development of closed-loop feedback control for station keeping has the potential to increase the safety, robustness, and reliability of satellites while also reducing operational costs [6], [20]. An MPC policy for the purpose of simultaneous station keeping, attitude control, and momentum management for a GEO satellite was developed in this paper. The satellite configuration, consisting of two

boom-thruster assemblies on the anti-nadir face, allows for more control action in the North-South direction compared to a previous configuration [7], which is desirable for station keeping. The introduction of a pulse-width modulation scheme in conjunction with a closed-loop MPC policy allows for physically realizable on-off thruster commands and satisfies all control objectives in simulation, including station keeping and attitude constraints.

REFERENCES

- [1] E. Y. Choueiri, "New dawn for electric rockets," *Scientific American*, vol. 300, no. 2, pp. 58–65, 2009.
- [2] J. Climer, "Boeing: World's first all-electric propulsion satellite begins operations," <http://boeing.mediaroom.com/index.php?s=20295&item=129516>.
- [3] J. J. Delgado, J. A. Baldwin, and R. L. Corey, "Space systems local electric propulsion subsystem: 10 years of on-orbit operation," in *30th International Symposium on Space Technology and Science*, 2015.
- [4] M. Martinez-Sanchez and J. E. Pollard, "Spacecraft electric propulsion – an overview," *Journal of Propulsion and Power*, vol. 14, no. 5, pp. 688–699, 1998.
- [5] A. Sukhanov and A. Prado, "On one approach to the optimization of low-thrust station keeping manoeuvres," *Advances in Space Research*, vol. 50, no. 11, pp. 1478 – 1488, 2012.
- [6] A. Weiss, U. Kalabic, and S. Di Cairano, "Model predictive control for simultaneous station keeping and momentum management of low-thrust satellites," in *Proc. 2015 American Control Conference*, pp. 2305–2310, 2015.
- [7] A. Walsh, S. Di Cairano, and A. Weiss, "MPC for coupled station keeping, attitude control, and momentum management of low-thrust geostationary satellites," in *American Control Conference (ACC), 2016*, pp. 7408–7413, American Automatic Control Council (AACC), 2016.
- [8] M. Leomanni, A. Garulli, A. Giannitrapani, and F. Scortecci, "All-electric spacecraft precision pointing using model predictive control," *Journal of Guidance, Control, and Dynamics*, vol. 38, no. 1, pp. 161–168, 2014.
- [9] D. Losa, M. Lovera, J.-P. Marmorat, T. Dargent, and J. Amalric, "Station keeping of geostationary satellites with on-off electric thrusters," in *Proc. 2006 IEEE International Conference on Control Applications*, pp. 2890–2895, 2006.
- [10] R. Vazquez, F. Gavilan, and E. F. Camacho, "Pulse-width predictive control for LTV systems with application to spacecraft rendezvous," *Control Engineering Practice*, 2016.
- [11] C. Gazzino, C. Louembet, D. Arzelier, N. Jozefowicz, D. Losa, C. Pittet, and L. Cerri, "Integer programming for optimal control of geostationary station keeping of low-thrust satellites," 2016.
- [12] B. M. Anzel, "Method and apparatus for a satellite station keeping," U.S. Patent 5 443 231, August 22, 1995.
- [13] R. L. Corey and D. J. Pidgeon, "Electric propulsion at space systems/loral," in *Proc. 31st International Electric Propulsion Conference, paper IEPC-2009-270*, 2009.
- [14] D. A. Herman, "Nasa's evolutionary xenon thruster (next) project qualification propellant throughput milestone: Performance, erosion, and thruster service life prediction after 450 kg," 2010.
- [15] P. C. Hughes, *Spacecraft Attitude Dynamics*. Mineola, New York: Dover Publications Inc., 2004.
- [16] J. Rawlings and D. Mayne, *Model predictive control: Theory and Design*. Madison, WI: Nob Hill Publishing, LLC, 2002.
- [17] S. Di Cairano, M. Brand, and S. A. Bortoff, "Projection-free parallel quadratic programming for linear model predictive control," *International Journal of Control*, vol. 86, no. 8, pp. 1367–1385, 2013.
- [18] A. Weiss, I. Kolmanovsky, D. S. Bernstein, and A. Sanyal, "Inertia-free spacecraft attitude control using reaction wheels," *Journal of Guidance, Control, and Dynamics*, vol. 36, no. 5, pp. 1425–1439, 2013.
- [19] A. H. J. de Ruiter, C. J. Damaren, and J. R. Forbes, *Spacecraft Dynamics and Control: An Introduction*. Chichester, West Sussex, U.K.: John Wiley & Sons, Ltd, 2013.
- [20] J. R. Wertz and W. J. Larson, eds., *Spacecraft Mission Analysis and Design*. Microcosm Press, 3rd ed., 1999.